CORROSION SCIENCE AND TECHNOLOGY, Vol.16, No.4(2017), pp.167~174
[Research Paper]
pISSN: 1598-6462 / eISSN: 2288-6524
DOI: https://doi.org/10.14773/cst.2017.16.4.167

Inhibition of Rebar Corrosion by Carbonate and Molybdate Anions

Y. T. Tan[1,†], S. L. Wijesinghe[2], and D. J. Blackwood[3]

[1]*NUS Graduate School for Integrative Sciences & Engineering, Centre for Life Sciences (CeLS), #05-01, 28 Medical Drive, Singapore 117456*
[2]*SIMTech, 71 Nanyang Drive, Singapore 638075*
[3]*National University of Singapore, 9 Engineering Drive 1, Singapore 117576*

(Received February 08, 2017; Revised February 08, 2017; Accepted August 17, 2017)

Bicarbonate/carbonate and molybdate anions have been characterized for their inhibitive effect on pitting corrosion of carbon steel in simulated concrete pore solution by using electrochemical tests such as electrochemical impedance (EIS) and linear polarization (LP). It was revealed that bicarbonate/carbonate has a weak inhibitive effect on pitting corrosion that is approximately one order of magnitude lower compared to hydroxide. Molybdate is effective against pitting corrosion induced by the concentration of chloride as low as 113 mM and can increase the pitting potential of a previously pitted sample to the oxygen evolution potential by the concentration of molybdate as much as 14.6 mM only. The formation of a $CaMoO_4$ film on the surface hinders the reduction of dissolved oxygen on the steel surface, reducing corrosion potential and increasing the safety margin between corrosion potential and pitting potential further. In addition, pore-plugging by $FeMoO_4$ as a type of salt film within pits increases the likelihood of repassivation.

Keywords: *steel, concrete, passivity, corrosion inhibitor, EIS*

1. Introduction

Bicarbonate/carbonate ions are generated in the process of carbonation of the concrete pore solution. Carbonation results in a decrease in the alkalinity of the pore solution and leads to a destabilization of the passive layer on the rebar surface. Along with chloride ingress, carbonation is one of the major causes of rebar corrosion [1,2].

Molybdate is a non-oxidizing anodic inhibitor for Fe and Al corrosion [3,4]. Although molybdate compounds have been recommended for use as corrosion inhibitors in concrete, this suggestion has not been taken up by the concrete industry [5]. Even though there have been some research investigating molybdate's effectiveness as a corrosion inhibitor for concrete rebars [6–9], there is a relative lack of information compared to that for calcium nitrite, which is currently the most widely used inhibitor for concrete rebars.

This work investigates the inhibitive effect of bicarbonate/carbonate and molybdate anions on pitting corrosion of carbon steel in reinforced concrete.

† Corresponding author: a0040270@nus.edu.sg

2. Experimental Procedure

Flat low-carbon steel specimens of grade AISI 1020 with dimensions 20 mm x 20 mm x 2 mm were used in this work and had a nominal composition in wt%: 0.20 C; 0.25 Si; 0.45 Mn; 0.04 P; 0.04 S; balance Fe. Before each experiment, the metal sample was ground with SiC papers from grade P180 to P600, degreased with ethanol, washed with deionized water and then blown dry with compressed air at room temperature. The abraded surface was then covered with a piece of electrochemical mask to prevent crevice corrosion and expose a well-defined circular area of 1 cm^2 to the electrolyte.

The simulated concrete pore solution was a saturated $Ca(OH)_2$ solution with a pH of 12.5 at room temperature. Chloride ingress was simulated by addition of NaCl and the pH drop caused by carbonation was simulated by the addition of $NaHCO_3$. Immediately before each experiment, 100 ml of electrolyte was prepared using deionized water and reagent-grade chemicals. The sample electrolyte was sparged with compressed N_2 gas for at least 30 minutes to deaerate it prior to the start of the electrochemical experiments.

Electrochemical experiments were conducted using a standard three-electrode set-up in an electrochemical cell and results were registered by a Solartron Analytical SI

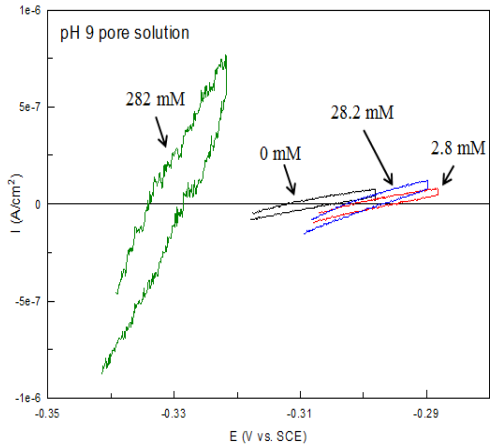

Fig. 1 LPR plots of AISI 1020 carbon steel in pH 9 pore solution with various chloride concentrations.

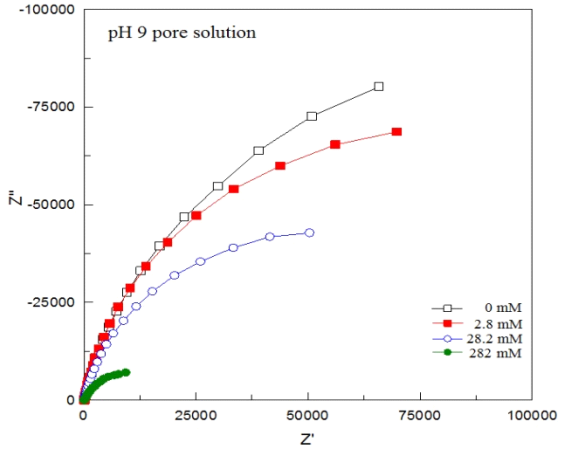

Fig. 2 EIS plots of AISI 1020 carbon steel in pH 9 pore solution with various chloride concentrations.

1287 potentiostat controlled by CorrWare software. Electrochemical impedance spectroscopy (EIS) experiments were carried out using a SI 1260 Impedance/Gain-phase Analyser in conjunction with the SI 1287. The working electrode was the carbon steel sample while the counter electrode was a high-density graphite rod. The reference electrode used was Hg/HgO/1.0 M NaOH (XR400 from Radiometer Analytical) that has a potential of +0.140 V vs. SHE, however, potentials quoted in this work are given with respect to the saturated calomel electrode (SCE) scale for easier comparison with the bulk of the literature. The electrochemical cell was placed in a Faraday cage to minimize electromagnetic noise. All experiments were conducted at ambient temperature (~23 °C).

For the LPR measurement, the metal sample was swept at 0.17 mV/s from −10 mV to +10 mV relative to its corrosion potential and there the sweep direction was reversed. The EIS experiment was conducted at the corrosion potential with an AC signal having an amplitude of 10 mV peak to peak, from 10 kHz to 10 mHz. Potentiodynamic polarisation curves were obtained from a starting potential of −0.9 V vs. SCE to a final potential of 0.95 V vs. SCE at a scan rate of +0.67 mV/s. Mott-Schottky plots were generated for 20 hour immersion experiments by using the imaginary part of the impedance at 1000 Hz from the EIS data.

In order to assess the inhibitive effect of molybdate on the different stages of pitting, a more complex testing regime was adopted in which the potentiodynamic scan started from the open-circuit corrosion potential determined at the end of 50 minutes after immersion and the potential was swept in a positive direction until pitting initiated as indicated by the current density reaching 1 mA/cm^2. This was then followed by either a potentiostatic or galvanostatic hold for 5 minutes to further propagate the localised attack. The carbon steel was then allowed to recover at open-circuit for 50 minutes before a second potentiodynamic polarisation scan was carried out, from −0.9 V vs. SCE to 0.95 V vs. SCE.

Scanning electron microscopy (SEM) and energy dispersive spectroscopy (EDS) were carried out using a Philips XL30 FEG SEM in secondary electron imaging mode with an accelerating voltage between 5 kV and 25 kV.

3. Results and Discussion

3.1 Inhibitive effect of bicarbonate and carbonate anions

Bicarbonate/carbonate ions are naturally generated during the process of carbonation and are present in greater amounts in pore solutions with lower pH values. In this work, different amounts of $NaHCO_3$ were added to the standard stock solution (saturated $Ca(OH)_2$ solution) in order to produce simulated pore solutions of different pH values. Three carbonated concrete pore solutions of pH 9, 10 and 11, which contain total bicarbonate and carbonate concentrations of 264, 47.3 and 29.4 mM respectively, were tested along with a pH 12.5 pore solution containing 31.6 mM OH^-, representing an uncarbonated condition.

The corrosion potential (measured after half an hour of immersion) at low chloride concentrations was dependent on pH value in an almost Nernstian manner, being around −0.3 V vs. SCE and −0.5 V vs. SCE for pH 9 and pH 12.5 pore solutions respectively. For all the pore solutions, the corrosion potential was lower at higher chloride concentrations.

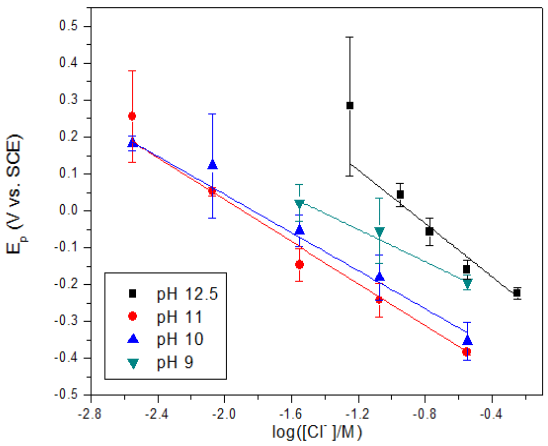

Fig. 3 Pitting potential of AISI 1020 carbon steel in different pore solutions against log [Cl⁻].

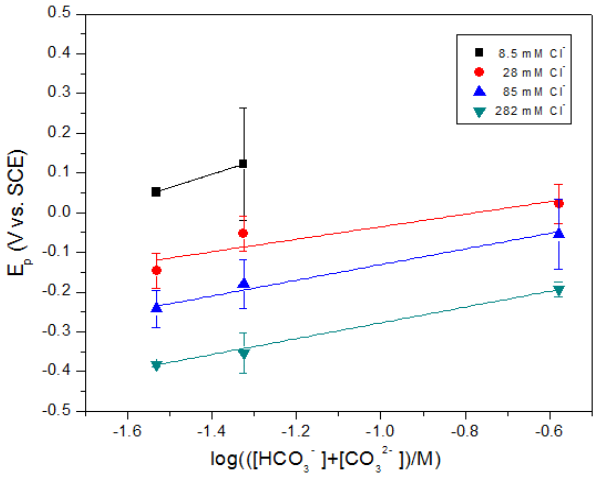

Fig. 4 Pitting potential of AISI 1020 carbon steel vs. log ($[HCO_3^-]+[CO_3^{2-}]$) at four different $[Cl^-]$.

Polarisation resistance (R_p) was measured using LPR and EIS after half an hour of immersion. The R_p values from LPR and EIS were in good agreement with each other, with the value from LPR being slightly lower due to the scan rate being slightly too fast (greater than the characteristic frequency) such that the capacitance of the system was exerting a non-negligible influence. Examples of LPR and EIS Nyquist plots are shown in Fig. 1 and Fig. 2 respectively.

The R_p was around 150 kΩ cm^2 for pH 12.5 pore solutions regardless of chloride concentration while it was around 100 kΩ cm^2 for the carbonated pore solutions at low chloride concentrations and decreased at higher chloride concentrations. At high chloride concentrations, R_p was higher in pH 9 pore solution by about a factor of two compared to pH 10 and 11 pore solutions, an indication that the bicarbonate/carbonate anions had a weak inhibitive effect on the corrosion rate.

In Fig. 3, pitting potentials (E_p) from potentiodynamic polarisation tests (for chloride concentrations higher than the critical chloride threshold concentration) decreased with increasing chloride concentration for all the pore solutions tested, and followed a linear relationship with the logarithm of the chloride concentration [10–12] as shown in Eq. 1. Pitting potential was in general highest for pH 12.5, followed by pH 9, 10 and finally pH 11 pore solution for a given chloride concentration.

$$E_p = a - b\log[Cl^-] \quad (1)$$

When the pitting potential was plotted against the logarithm of the bicarbonate/carbonate concentration for the carbonated pore solutions at four selected chloride concentrations, there was an obvious increase in pitting potential with increasing bicarbonate/carbonate concentration (Fig. 4).

The critical $[Cl^-]/[OH^-]$ ratio for pitting of pH 12.5 pore solution and the critical $[Cl^-]/([HCO_3^-]+[CO_3^{2-}])$ ratio of pH 9, 10 and 11 pore solutions are shown in Fig. 5. It can be seen that the critical $[Cl^-]/([HCO_3^-]+[CO_3^{2-}])$ ratio is around one order of magnitude lower compared to the critical $[Cl^-]/[OH^-]$ ratio. This is further corroborated by calculations using data in Fig. 3 and Fig. 4 that show that the amount of bicarbonate/carbonate anions required to obtain the same pitting potential exhibited by carbon steel in the presence of 31.6 mM OH^- for a given chloride concentration is more than 10 times higher than the hydroxide concentration, with the inhibitive factor (defined in Eq. 2) approaching 10^{-1} with increasing chloride concentration (Fig. 6). Therefore, bicarbonate/carbonate anions have an inhibitive effect on pitting corrosion, albeit a weak one compared to that exhibited by hydroxide anions.

$$Inhibitive\ factor_{[Cl^-]=x} = \frac{[OH^-]_{[Cl^-]=x}}{[[HCO_3^-]+[CO_3^{2-}]]_{[Cl^-]=x}} \quad (2)$$

The data here suggest that in real concrete systems, corrosion due to carbonation in the presence of chloride could have been worse if not for the inhibitive effect of bicarbonate/carbonate anions generated in the carbonation process.

3.2 Inhibitive effect of molybdate anion

Molybdate anions were tested as corrosion inhibitors for protection against pitting corrosion in pH 12.5 pore solutions containing 113 mM and 564 mM Cl^-, represent-

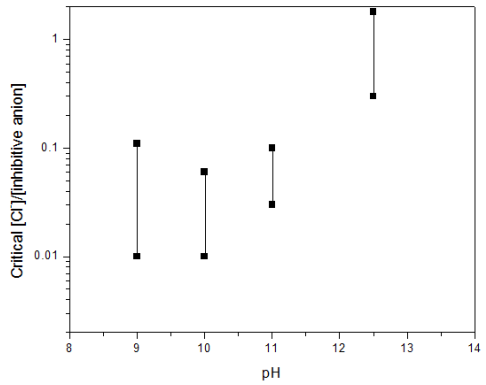

Fig. 5 Critical $[Cl^-]/[OH^-]$ ratio for pH 12.5 pore solution and critical $[Cl^-]/([HCO_3^-]+[CO_3^{2-}])$ ratio for pH 9, 10 and 11 pore solutions.

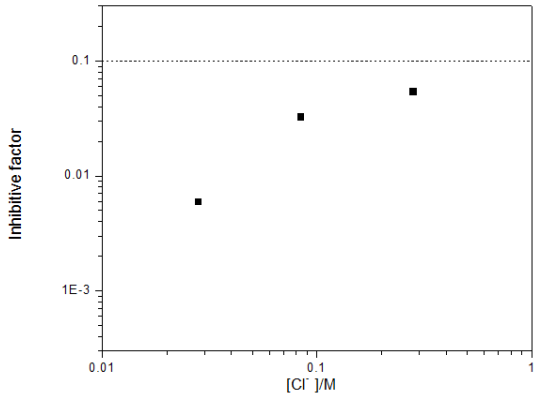

Fig. 6 Inhibitive factor (relative inhibitive effectiveness of bicarbonate/carbonate vs. hydroxide) calculated from pitting potential data at different chloride concentrations.

ing light and severe chloride contamination respectively. These chloride concentration values were chosen for testing as they were higher than the critical chloride threshold concentration for pH 12.5 pore solution (as determined above) and thus gave reproducible pitting potentials with sample standard deviations of around 30 mV.

In order to assess the effect of molybdate on the different stages of pitting corrosion, a more complicated experimental procedure was adopted. After 50 minutes of immersion, a potentiodynamic polarisation scan was used to initiate localized attack on the steel surface by doing a positive potential sweep from the corrosion potential until the potential where the current density was 1 mA/cm^2. Since the current density in the passive region was on the order of 1 $\mu A/cm^2$, a current density of 1 mA/cm^2 represents a state in which pitting has occurred. This was then followed by either a potentiostatic hold at this potential or a galvanostatic hold at 1 mA/cm^2 to grow the attack. The carbon steel was then allowed to recover for 50 minutes before a second potentiodynamic polarisation scan was then carried out from −0.9 V vs. SCE to 0.95 V vs. SCE.

The molybdate anions were introduced at one of two different times: either at the start of the experiment or after the potentiostatic/galvanostatic hold when localized corrosion had already occurred.

In general, the current density increased throughout the duration of the 5 minutes of potentiostatic experiment (Fig. 7) while the potential measured during the 5 minutes of galvanostatic experiment decreased with time (Fig. 8).

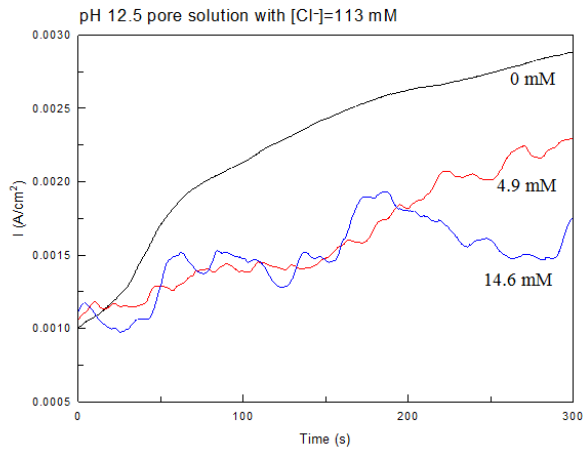

Fig. 7 Current density during potentiostatic hold for AISI 1020 carbon steel in pH 12.5 pore solution with 113 mM Cl^- and various molybdate concentrations.

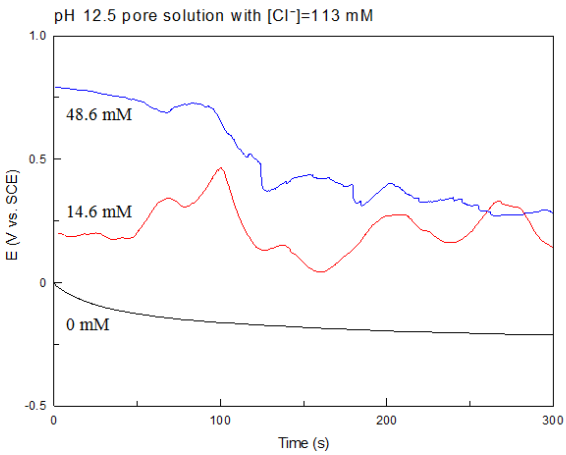

Fig. 8 Electrode potential during galvanostatic hold for AISI 1020 carbon steel in pH 12.5 pore solution with 113 mM Cl^- and various molybdate concentrations.

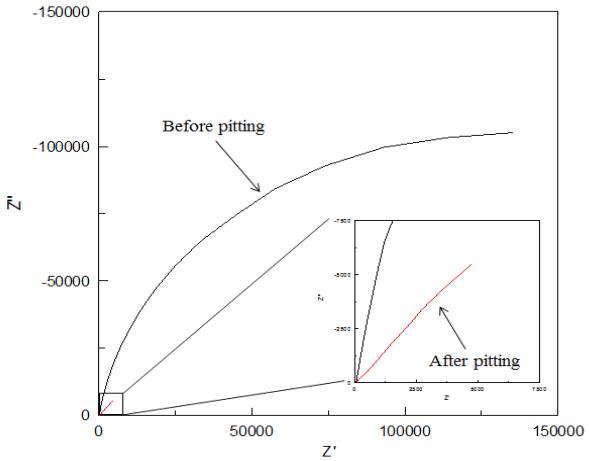

Fig. 9 Nyquist plots showing a change in impedance behaviour after pitting for AISI 1020 carbon steel in pH 12.5 pore solution with 113 mM Cl^- and 14.6 mM MoO_4^{2-}.

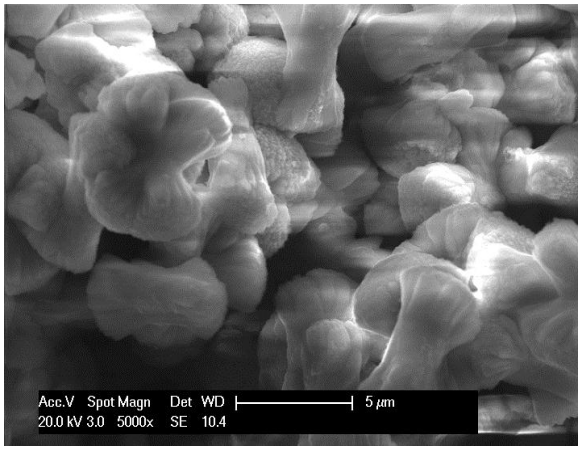

Fig. 10 $CaMoO_4$ film formed on AISI 1020 carbon steel surface when $[MoO_4^{2-}] \geq$ 48.6 mM.

These observations are consistent with expectations since the anodic dissolution rate is expected to increase sharply after pitting has occurred. Thus a given current density can be achieved at a lower potential than before, while at a given potential, the current density will be higher than before. It was also observed that the potentiostatic hold method led to more severe pitting corrosion compared to the galvanostatic hold method, as seen from the lower pitting potential in the second potentiodynamic sweep. This is because the total propagation was higher for the potentiostatic hold experiment by virtue of its higher total charge passed.

Half an hour after the initiation and growth of the localized attack, the corrosion potential was up to 200 mV lower (from −0.5 V vs. SCE to −0.7 V vs. SCE) compared to that measured in the first part of the experiment while the carbon steel was still in the passive state. This was true for both chloride concentrations (113 mM and 564 mM Cl^-) and is an indication that the previous attacked site did not fully repassivate during the period of recovery before the next potentiodynamic scan. It was noted that the presence of molybdate did not affect the corrosion potential of active systems significantly.

The R_p after the occurrence of localized corrosion could be up to one order of magnitude lower compared to that before, being more than 100 kΩ cm^2 for passive systems and around 10 kΩ cm^2 for pitted systems. EIS data (Fig. 9) showed that the impedance of the steel was then dominated by mass transport, with the exponent of the constant phase element (CPE) being ≤ 0.7, which is indicative of diffusion control across pit covers [13].

The presence of molybdate at high concentrations ($[MoO_4^{2-}] \geq$ 48.6 mM) can help to increase R_p of carbon steels in the passive state by forming a $CaMoO_4$ film (identity confirmed by EDS) on the carbon steel surface (Fig. 10), though it was observed that it takes a few hours for this precipitated film to completely cover the steel surface. The R_p after pitting was not significantly improved by the presence of molybdate anions.

In the absence of molybdate, the (first) pitting potential of carbon steel in pH 12.5 pore solution with 113 mM Cl^- was around −0.02 V vs. SCE with a sample standard deviation of 30 mV. When the chloride concentration was 564 mM, the pitting potential was −0.21 V vs. SCE with a sample standard deviation of 20 mV. The pitting potential was virtually independent of whether the potentiodynamic scan started from the corrosion potential or from −0.9 V vs. SCE.

It was observed that the addition of molybdate to chloride-contaminated pore solution before the start of the experiment was able to increase the (first) pitting potential of the carbon steel, with the increase being larger for higher molybdate concentration. For pH 12.5 pore solution containing 113 mM Cl^-, the presence of 146 mM MoO_4^{2-} increased the (first) pitting potential by more than 300 mV (Fig. 11). For pH 12.5 pore solution containing 564 mM Cl^-, the addition of molybdate (up to 146 mM) to the pore solution increased the (first) pitting potential only negligibly, with the pitting potential being the same within the limits of experimental error (Fig. 12).

A comparison of the pitting potential from the first and second potentiodynamic polarisation scans showed that the second pitting potential was in general higher than the first. This was true even in the absence of molybdate, though the presence of molybdate increased the second pitting potential much more. For the pore solution with

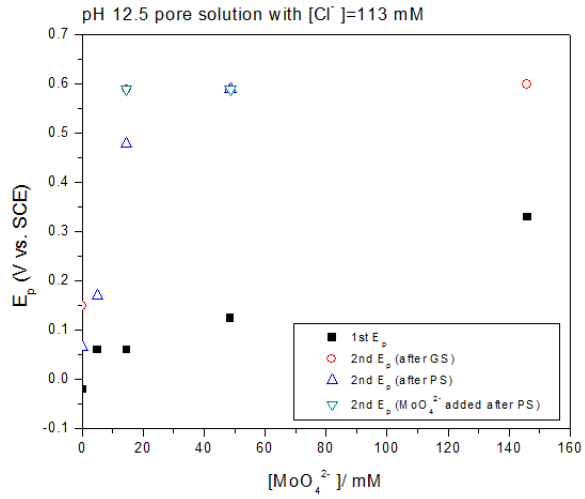

Fig. 11 Pitting potentials of AISI 1020 carbon steel vs. molybdate concentration for [Cl⁻] =113 mM. GS and PS represent galvanostatic hold and potentiostatic hold respectively.

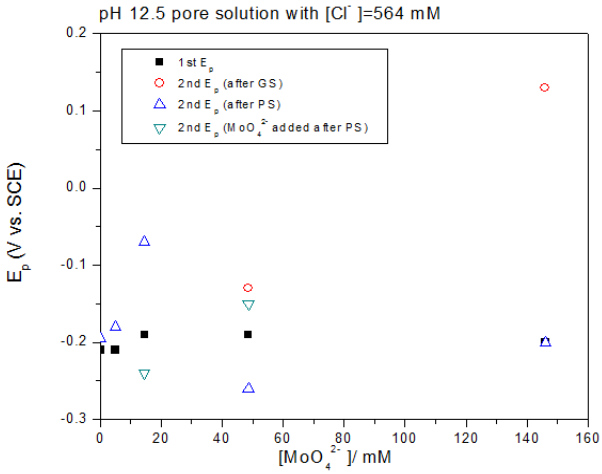

Fig. 12 Pitting potentials of AISI 1020 carbon steel vs. molybdate concentration for [Cl⁻] =564 mM. GS and PS represent galvanostatic hold and potentiostatic hold respectively.

113 mM Cl^-, $[MoO_4^{2-}] \geq 14.6$ mM was sufficient to raise the pitting potential in the second potentiodynamic scan to 0.59 V vs. SCE, which is the oxygen evolution potential for pH 12.5 pore solution; i.e. pitting was effectively eliminated. In the presence of 564 mM Cl^-, the pitting potential from the second potentiodynamic scan was only marginally higher in all cases with the exception of that observed for 146 mM MoO_4^{2-} (galvanostatic hold), where there was significant increase in pitting potential by 300 mV.

Therefore, molybdate is effective against pitting corrosion at lower chloride contamination levels, it being shown that for carbon steel that has previously suffered pitting, the addition of molybdate above a critical amount is able to raise the subsequent pitting potential to the oxygen evolution potential.

It is interesting to note that even without molybdate, the second pitting potential was higher than the first for pH 12.5 pore solution containing 113 mM Cl^-, while no difference was observed (within the limits of experimental error) for the pore solution with 564 mM Cl^-. This means that the pit was able to repassivate during the initial part of the second potentiodynamic scan, helped by starting the second scan at −0.9 V vs. SCE, which was 200 mV lower than the typically observed corrosion potential after pitting has occurred. This repassivation could not have taken place during the 50 minutes of recovery time between the first and second potentiodynamic sweep since R_p measured during this recovery period was much lower than that observed for the passive state.

Given that the first potentiodynamic sweep had caused the initiation of pits at the most susceptible sites (lowest pitting potential), the fact that the second potential sweep had to reach a higher potential before the next set of susceptible sites could be activated or for the previously active sites to be reactivated implies the repassivation at the initial part of the subsequent potentiodynamic scan was very successful.

It has previously been recognized that the dispersion in pitting potential is lower at higher chloride concentrations [14]. A higher chloride concentration makes the different possible pit initiation sites present on a metal surface increasingly equal in terms of pitting susceptibility. This may explain why there was no significant difference between the first and second pitting potentials for pH 12.5 pore solution with 564 mM Cl^-, since the next set of susceptible sites has only a marginally higher pitting potential.

3.3 Comparison of mechanisms of inhibition between bicarbonate/carbonate and molybdate

There are a few possible mechanisms of inhibition by the bicarbonate/carbonate ions.

Firstly, a $FeCO_3$ outer layer could have formed via precipitation that protects the underlying metal substrate. However, the presence of such a film could not be confirmed by SEM and EDX in practice. If a $FeCO_3$ film did indeed form, it could have been further oxidized to a ferrous/ferric oxide film [15]. Another possibility is that the $FeCO_3$ film was not adherent to the steel surface and was thus washed away along with other corrosion products during the cleaning process at the end of the electrochemical experiment.

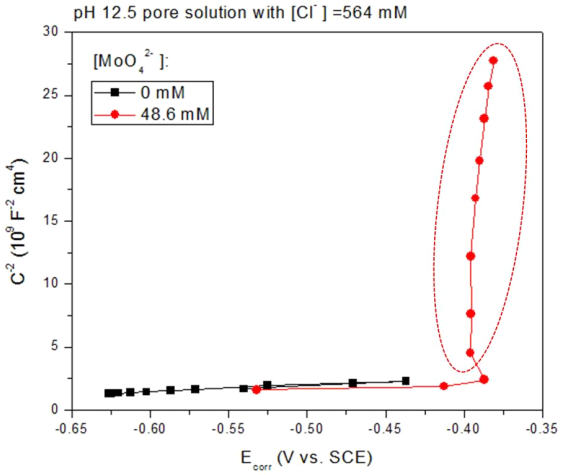

Fig. 13 Mott-Schottky plots for AISI 1020 carbon steel with 564 mM Cl^-. Circled region refers to data collected after formation of $CaMoO_4$ film. Note the initial decrease in E_{corr} right after complete formation of the outer layer.

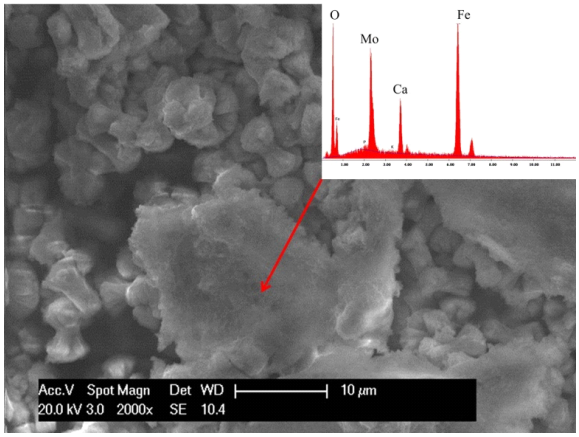

Fig. 14 Incorporation of Mo in corrosion products found within pits.

A second possible mechanism is competitive adsorption of bicarbonate/carbonate ions with chloride at the barrier layer/solution interface such that a higher bulk chloride concentration is required for a critical adsorbed chloride concentration on the metal surface. This mechanism will mostly protect against pitting by delaying pit initiation. A third mechanism is that once pit initiation has occurred, electromigration of bicarbonate/carbonate ions into the nascent pit can help retard the rate of localized acidification within the pit due to the buffering capacity of bicarbonate/carbonate anions, thus hindering the pit propagation rate. By constituting part of the ionic current that moves into the pit to maintain charge neutrality, bicarbonate/carbonate anions also help to raise the pitting potential by requiring a higher electrode potential before sufficient chloride ions are accumulated within the pit.

The proposed mechanisms for the inhibitive effect of molybdate anions are similar to those suggested for bicarbonate/carbonate, namely competitive adsorption with chloride on the steel surface, the formation of a precipitated outer layer and electromigration into nascent pits so as to maintain charge neutrality.

However, in comparison to bicarbonate/carbonate, the precipitated film formed by molybdate is adherent to the steel surface. This calcium molybdate film serves to restrict oxygen access to the steel surface, thus leading to a retardation of the cathodic reaction rate. This explanation is supported by a separate set of experiments where carbon steel samples were monitored over 20 hours of immersion; lower corrosion potential and higher R_p were observed for systems after developing this calcium molybdate film. Mott-Schottky analysis showed that the donor density decreased by more than three orders of magnitude after the development of a precipitated outer layer at higher molybdate concentrations (Fig. 13).

Similar to the case of bicarbonate/carbonate, molybdate may also reduce the rate of chloride migration into the pit by constituting part of the ionic current that moves into the pit to restore electroneutrality. However, molybdate does not act as a buffer unlike bicarbonate/carbonate. In addition, molybdate precipitates out of the solution within the pit after reacting with the high Fe^{2+} concentration since $FeMoO_4$ is insoluble in aqueous solutions (Fig. 14). This repassivation of the active site by a $FeMoO_4$ salt film has been termed as a pore–plugging mechanism by other researchers [16].

Thus molybdate can reduce the corrosion current density by depressing the cathodic reaction rate and protects against pitting by both decreasing the corrosion potential and increasing the pitting potential, which delays the onset of pitting by increasing the safety margin between the corrosion potential and the pitting potential.

Comparing bicarbonate/carbonate with molybdate, it can be seen that their inhibition mechanisms are somewhat different, with molybdate being the more effective inhibitor due to its ability to precipitate out within pits to bring about repassivation and requiring a smaller critical concentration to be effective. A more detailed comparison awaits further experimental data that are in the midst of being collected.

4. Conclusions

The inhibitive effect of bicarbonate/carbonate and molybdate anions have been characterised for pitting corrosion of carbon steel in simulated concrete pore solution. Bicarbonate/carbonate anions have a weak inhibitive effect on pitting corrosion that is around one order of magnitude lower than hydroxide. Corrosion of carbon steel in carbonated pore solution with reduced alkalinity would have been worse but for this weak inhibitive effect by the anions generated in the process of carbonation.

Molybdate was effective in raising the pitting potential of carbon steel in pH 12.5 pore solution with 113 mM Cl^-. Addition of at least 14.6 mM MoO_4^{2-} was able to increase the pitting potential of a previously pitted sample to the oxygen evolution potential, i.e. effectively eliminating pitting. Formation of a $CaMoO_4$ film on the surface hinders the reduction of dissolved oxygen on the steel surface, reducing the corrosion potential and increasing the safety margin between the corrosion potential and the pitting potential further. Pore-plugging by $FeMoO_4$ within pits increases the likelihood of repassivation.

Acknowledgments

Y. T. Tan acknowledges the support of a NUS Graduate School (NGS) scholarship. Financial support for this project was provided by Singapore Institute of Manufacturing Technology (SIMTech) under project No. U12-S-036SU.

References

1. S. Mindess, J. F. Young, and D. Darwin, *Concrete,* 2nd ed., pp. 1-644, Prentice Hall PTR, USA (2003).
2. C. L Page and M. M. Page, *Durability of Concrete and Cement Composites*, 1st ed., pp. 136–186, Woodhead Publishing Limited, Cambridge (2007).
3. M. S. Vukasovich and D. R. Robitaille, *J. Less Common Met.*, **54**, 437 (1977).
4. M. S. Vukasovich and J. P. G. Farr, *Polyhedron*, **5**, 551 (1986).
5. V. S. Ramachandran, *Concrete Admixtures Handbook*, 2nd ed., pp. 878–938, Wiilliam Andrew, New York (1996).
6. B. B. Hope and A. K. C. Ip, *Proc. International RILEM Symposium*, pp. 299–306, Chapman and Hall, UK (1990).
7. Y. Tang, G Zhang, and Y. Zuo, *Constr. Build. Mater.*, **28**, 327 (2012).
8. M. A. G. Tommaselli, N. A. Mariano, and S. E. Kuri, *Constr. Build. Mater.*, **23**, 328 (2009).
9. S. M. Abd El Haleem, S. Abd El Wanees, E. E. Abd El Aal, and A. Diab, *Corros. Sci.*, **52**, 292 (2010).
10. N. Azzerri, F. Mancia, and A. Tamba, *Corros. Sci.*, **22**, 675 (1982).
11. M. G. Alvarez and J. R. Galvele, *Corros. Sci.*, **24**, 27 (1984).
12. J. R. Galvele, *J. Electrochem. Soc.*, **123**, 464 (1976).
13. G. S. Frankel, *J. Electrochem. Soc.*, **145**, 2186 (1998).
14. Y. Zhang, M. Urquidi-Macdonald, G. R. Engelhardt, and D. D. Macdonald, *Electrochim. Acta*, **69**, 12 (2012).
15. D. H. Davies and G. T. Burstein, *Corrosion*, **36**, 416 (1980).
16. J. Sinko, *Prog. Org. Coat.*, **42**, 267 (2001).